



QUANTITATIVE ASSESSMENT OF REGIONAL PULMONARY PERFUSION USING THREE-DIMENSIONAL ULTRAFAST DYNAMIC CONTRAST-ENHANCED MAGNETIC RESONANCE IMAGING: PILOT STUDY RESULTS IN 10 PATIENTS

© Anna V. Zakharova^{1,2}, Victoria V. Pritz³, Alexander V. Pozdnyakov^{1,4}

¹ St. Petersburg State Pediatric Medical University, Saint Petersburg, Russia;

² City Multidisciplinary Hospital No. 2, Saint Petersburg, Russia;

³ City Mariinsky Hospital, Saint Petersburg, Russia;

⁴ Academician A.M. Granov Russian Scientific Center for Radiology and Surgical Technologies, Saint Petersburg, Russia

For citation: Zakharova AV, Pritz VV, Pozdnyakov AV. Quantitative assessment of regional pulmonary perfusion using three-dimensional ultrafast dynamic contrast-enhanced magnetic resonance imaging: pilot study results in 10 patients. *Pediatrician (St. Petersburg)*. 2021;12(6):15-26. <https://doi.org/10.17816/PED12615-26>

Received: 19.10.2021

Revised: 17.11.2021

Accepted: 29.12.2021

Background. Currently there is a high demand in reliable noninvasive diagnostic technique assessing the physiological parameters of the lungs. We are exploring the three-dimensional ultrafast MRI sequence as a novel diagnostic modality allowing the assessment of regional quantitative perfusion parameters in pulmonary tissue.

Aim. To assess regional differences in quantitative pulmonary perfusion parameters in 10 volunteers with no evidence of interstitial lung disease by computed tomography, clinical, and laboratory data.

Materials and methods. 10 volunteers with no signs of interstitial lung disease were examined by three-dimensional ultrafast dynamic contrast-enhanced MR imaging using 3D T1-weighted images. The values of pulmonary blood flow (PBF), mean transit time (MTT), and pulmonary blood volume (PBV) for the targeted regions of interest were calculated based on the dynamic image series. For calculations, arterial input function (AIF) was used, as well as the time-intensity curves.

Results. The values of PBF, MTT, and PBV showed statistically significant differences between central and peripheral sections of lungs. Provided model can be implemented for quantitative assessment of regional pulmonary perfusion allows it to be used to determine the reliability of PBF, MTT and PBV values.

Conclusions. Three-dimensional ultrafast MRI sequence is a novel diagnostic modality allowing the assessment of regional quantitative pulmonary perfusion parameters in pulmonary tissue, regardless of physiological features of blood supply mechanisms in different lung regions.

Keywords: lung; magnetic resonance; MR; perfusion; gadolinium; dynamic contrast enhancement.

ВОЗМОЖНОСТИ КОЛИЧЕСТВЕННОЙ ОЦЕНКИ РЕГИОНАРНОЙ ЛЕГОЧНОЙ ПЕРФУЗИИ С ИСПОЛЬЗОВАНИЕМ ТРЕХМЕРНОЙ СВЕРХБЫСТРОЙ ДИНАМИЧЕСКОЙ КОНТРАСТНОЙ МАГНИТНО-РЕЗОНАНСНОЙ ТОМОГРАФИИ: ПРЕДВАРИТЕЛЬНЫЙ ОПЫТ У 10 ИСПЫТУЕМЫХ

© А.В. Захарова^{1,2}, В.В. Приц³, А.В. Поздняков^{1,4}

¹ Санкт-Петербургский государственный педиатрический медицинский университет, Санкт-Петербург, Россия;

² Городская многопрофильная больница № 2, Санкт-Петербург, Россия;

³ Городская Мариинская больница, Санкт-Петербург, Россия;

⁴ Российский научный центр радиологии и хирургических технологий им. акад. А.М. Гранова, Санкт-Петербург, Россия

Для цитирования: Захарова А.В., Приц В.В., Поздняков А.В. Возможности количественной оценки регионарной легочной перфузии с использованием трехмерной сверхбыстрой динамической контрастной магнитно-резонансной томографии: предварительный опыт у 10 испытуемых // Педиатр. – 2021. – Т. 12. – № 6. – С. 15–26. <https://doi.org/10.17816/PED12615-26>

Поступила: 19.10.2021

Одобрена: 17.11.2021

Принята к печати: 29.12.2021

Актуальность. В настоящее время ведется изучение новых и адаптация уже существующих методов лучевой диагностики для оценки физиологических параметров легких. Необходимы дальнейшие исследования методики трехмерной сверхбыстрой магнитно-резонансной томографии легких в качестве нового диагностического метода, позволяющего оценивать региональные количественные параметры перфузии в легочной ткани.

Цель исследования — оценить региональные различия в количественных параметрах легочной перфузии у 10 добровольцев, не имеющих признаков интерстициального поражения легких по данным компьютерной томографии, а также клинично-лабораторным данным.

Материалы и методы. Проведено обследование 10 добровольцев без признаков интерстициального поражения легких с применением трехмерной сверхбыстрой динамической контрастной магнитно-резонансной томографии на базе градиентных 3D-T1-взвешенных изображений. На основе динамических серий изображений получены значения PBF (скорость кровотока), PBV (объем кровотока) и MTT (среднее время пассажа) для выбранных областей интереса. Для вычислений использовали входную артериальную функцию AIF, а также кривые зависимости интенсивности от времени.

Результаты. Значения PBF, MTT и PBV показали достоверные различия между центральными и периферическими отделами легочных долей. Математическая модель, использованная при количественной оценке регионарной легочной перфузии, позволяет использовать ее для определения достоверности значений PBF, MTT и PBV.

Заключение. Трехмерная сверхбыстрая магнитно-резонансная последовательность позволяет количественно оценить перфузионные параметры для легочной ткани вне зависимости от физиологических особенностей механизмов кровоснабжения различных зон легких.

Ключевые слова: легкое; магнитный резонанс; МР; перфузия; гадолиний; динамическое контрастное усиление.

BACKGROUND

In pulmonary diseases, the preservation of blood flow with a decrease in the level of ventilation, the so-called perfusion–ventilation mismatch, becomes a common phenomenon [11]. Therefore, it is important to quantify perfusion and ventilation characteristics, both collectively and individually. The total values of these parameters are estimated by single-photon emission computed tomography combined with computed tomography (SPECT/CT) using radionuclide-labeled erythrocytes or serum albumin macroaggregates, Xe 133 and 15O-water [31, 36–38, 43]. However, perfusion can be assessed using contrast-enhanced dual-energy X-ray CT [45]. The implementation of both methods is associated with the use of ionizing radiation; in addition, these methods have a relatively low temporal resolution associated with the presence of the dead time of the detector, relatively low spatial resolution, and different energy resolution of ionizing radiation detectors.

Currently, several studies are describing the possibilities of two-dimensional dynamic contrast magnetic resonance imaging (MRI) to assess pulmonary blood flow (PBF) [17, 18, 25]. Compared with radioisotope studies, two-dimensional (2D) dynamic contrast-enhanced MR provides higher temporal and spatial resolution without the use of ionizing radiation. The 2D dynamic MR method represents a set of series of 2D-T1-weighted images. In this case, images are obtained continuously in a certain time interval after contrast agent injection. This method enables the assessment of the nature of accumulation at different time points. However, given the

requirements for temporal resolution, images have a low signal-to-noise ratio and low spatial resolution. In addition to these shortcomings, 2D dynamic contrast-enhanced MRI for lung examination does not allow simultaneous assessment of regional pulmonary perfusion due to field heterogeneity, which contributed to the further technical development and improvement of this technique [28].

Currently, new diagnostic capabilities of MRI are emerging, meet various physiological tasks, and consequently allow evaluation of many physiological parameters. The use of a dynamic series of three-dimensional (3D) T1-weighted sequences based on gradient echo with ultrashort repetition time (TR) and time to echo (TE) values enables data acquisition with the necessary temporal and spatial resolution for making perfusion maps [32, 33].

In the experimental works of several researchers [22, 29, 44], the concept of the first passage of a contrast agent was used as a physiological model for calculations, which has proven itself well for assessing the state of the central nervous system in ischemic or volumetric lesions of the brain. These works are characterized by the fact that the use of the gamma distribution was not acceptable when approximating the curve of signal intensity versus time. Some studies have shown that MR perfusion of the lungs with the calculation of quantitative parameters of blood flow is quite effective, which was confirmed in the porcine pulmonary embolism model [18, 19, 26].

In the present study, we extended this field-proven 2D technique to 3D ultrafast dynamic contrast-enhanced MRI in healthy volunteers.

This study aimed to quantify regional differences in pulmonary perfusion parameters in healthy volunteers using 3D ultrafast dynamic contrast-enhanced MRI with the calculation of PBF, mean transit time (MTT), and pulmonary blood volume (PBV) values.

MATERIALS AND METHODS OF RESEARCH

3D dynamic contrast-enhanced MRI [24] was performed on 10 healthy volunteers without a history of viral (COVID-19) pneumonia, and without chronic lung disease at the time of the study. The age of the patients at disease onset ranged from 24 to 58 (mean age, 38.5 ± 13.3) years. In all cases, the study started with a routine MRI of the lungs and then proceeded to the study using a gadolinium-containing contrast agent (Gadoteridol) [41].

Perfusion MRI was performed in the dynamic susceptibility contrast (DSC) mode, named 4D_LUNG_PERFUSION, representing a set of series of T1-weighted 3D sequences built on the basis of gradient-echo sequences oriented in the oblique-coronal plane (scans were oriented parallel to the sternum, taking into account the variants of the thoracic spine structure); the sequence parameters are presented in Table 1. The study area included all

parts of the lungs, namely, upper and lower on both sides, middle lobe of the right lung, and lingular lobes of the left lung.

By using the Medrad automatic injector, gadolinium-containing contrast agent gadoteriol at a concentration of 273.3 mg/mL and dose of 1.0 mL was injected to patients intravenously through an intravenous catheter 18 located in the antecubital fossa, with a constant injection rate of 3.5 mL/s and followed by the injection of 40 mL of isotonic sodium chloride solution at the same rate. During the first passage of the contrast agent bolus through the vascular system, images were repeatedly recorded at 40 different levels, with seven dynamic images obtained at each level. Images of the first passage were obtained before injection of a contrast agent to determine the baseline intensity of the MR signal. From the moment of contrast medium injection, the perfusion study took 18 s.

The following assumptions were used to estimate perfusion:

1) The selected region of interest (ROI) has one source and one drain for the contrast agent.

2) A large feeding vessel can be isolated, which enables the acquisition of the intensity–time dependence graph to obtain the corresponding input data.

Table 1 / Таблица 1

Technical parameters of the dynamic contrast susceptibility (DSC) MRI sequences on the Ingenia Philips 1.5 Tesla MR scanner

Характеристика параметров методики перфузионной магнитно-резонансной томографии в режиме динамической восприимчивости контраста на томографе Ingenia Philips 1,5 Тесла

Parameters / Параметры	4D_LUNG_PERFUSION
Orientation of slices / Ориентация срезов	Coronal / Корональная
Pulse sequence / Импульсная последовательность	TFE
TR/TE, ms / TR/TE, мс	3.5/1.57
Matrix / Матрица	132 × 117 × 40
Voxel size, mm (sag × tra × vert) / Размер вокселя, мм (сагитт × попер × верт)	3.03 × 2.99 × 8.00
Slice thickness, mm / Толщина среза, мм	4
NSA	1
Full scan time, sec / Полное время сканирования, с	18
Total number of series in the set / Общее количество серий в наборе	22
Time of the control scan with full filling of the k-space, sec / Время контрольного скана с полным заполнением k-пространства, с	2.5
Temporary resolution, sec / Временное разрешение, с	0.6

Note. In the physiological model for evaluating perfusion it is assumed that there is no “dead space” in the regions of interest [9], as well as arterial-venous shunts [7]. The contribution of intensity due to trophic blood flow (via bronchial arteries) [39] in this work is considered negligible and is not taken into account.

Примечание. При построении физиологической модели для оценки перфузии считается, что в исследуемой области отсутствует «мертвое пространство» [9], а также артериально-венозные шунты [7]. Вклад интенсивности за счет трофического кровотока [39] в данной работе считается пренебрежимо малым и не учитывается.

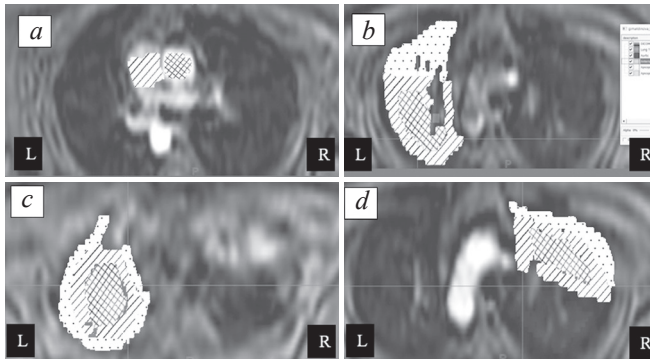


Fig. 1. Axial reconstructions of image with dynamic contrast enhancement. *a* – Selection of ROI in the area of the pulmonary trunk and ascending aorta for a qualitative assessment of the suitability of the data; *b, c* – Selection of areas of interest in the left lung: peripheral and central sections of the apical-posterior segment of the left lung at different levels are demonstrated; *d* – the same for the right lung with separate examination in the upper lobe of the apical and posterior segments. These are mirror images of classic-oriented CT/MRI projections

Рис. 1. Аксиальные реконструкции серий изображений с динамическим контрастным усилением. *a* – Выбор ROI в области легочного ствола и восходящего отдела аорты для качественной оценки пригодности данных; *b, c* – выбор зон интереса в левом легком: продемонстрированы периферические и центральные отделы верхушечно-заднего сегмента левого легкого на разных уровнях; *d* – то же для правого легкого с отдельным рассмотрением в верхней доле верхушечного и заднего сегментов. Следует обратить внимание, что данные изображения являются зеркально отраженными относительно классической ориентации компьютерных и магнитно-резонансных изображений

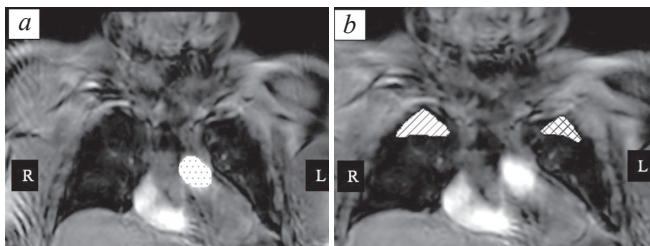


Fig. 2. Coronal reconstructions of image with dynamic contrast enhancement. *a* – The choice of ROI for AIF. When selecting this area of interest, MPR reconstructions should be used to exclude pulmonary arteries from the area of interest; *b* – selection of areas of interest in the coronal plane for comparison with the published data

Рис. 2. Корональные реконструкции серий изображений с динамическим контрастным усилением. *a* – Выбор ROI для определения функции AIF. При выборе данной области интереса следует использовать MPR-реконструкции для исключения из зоны интереса легочных артерий; *b* – выбор областей интереса в корональной плоскости для сравнения с приведенными в литературе данными

3) The resulting dependence graph should have sections of increase and decrease, and the intensity values at the zero and end points should be approximately equal, which would indicate the absence of the contrast agent accumulation.

To analyze the data obtained during the survey, two approaches were used, namely, qualitative approach that was based on numerical data on the dependence of intensity on time in the selected area of interest and semiquantitative approach with post-processing in the Firevoxel program, with subsequent data processing based on the MATLAB package [8] and its built-in functions.

The analysis was performed for the corresponding ROIs which were selected in two planes (Figs. 1, 2). The ROI was chosen while considering the blood supply to the apexes of the lungs, whereas segments of the apexes of the lungs were considered with a separate study of the central and peripheral zones.

First, the level of the pulmonary trunk and ascending aorta was examined to assess the reference function (Fig. 1, *a, b*). The criterion for selecting images was the absence of a peak in the curves of the dependence of the signal intensity on time, for example, in cases of earlier contrast enhancement or manifestation of individual physiological characteristics. Similarly, data obtained from four participants were excluded, and data of 10 volunteers were recognized as suitable for further analysis (14 volunteers examined in total).

Further, the zones of interest were selected in the apical segments from the level of the aortic arch and above with an interval of 1.5–2 cm, depending on the anthropometric parameters of the patient. In total, four levels were assessed, namely, the first at the level of the aortic arch, the last at the apex of the lung, without isolating the peripheral section.

Such a choice of the zone of interest is logically justified by the fact that the peripheral parts have less blood supply and should have a longer average passage time.

During subsequent postprocessing, relative and normalized values were obtained, as well as graphs of the dependence of the relative intensity.

In addition to the selection of the zone of interest described above, ROIs oriented in the coronal plane were considered. Such a choice of the area of interest reflects to a lesser extent the physiological characteristics of the blood supply to the lungs; therefore, this projection was used only to calculate the arterial input function (AIF).

The sufficiently large area of the ROI was due to the subsequent mathematical calculations required for function smoothness [20], and such an ROI en-

ables the smoothing of the curves of the intensity–time dependence by averaging the intensity over a large number of voxels.

Regional differences in mean PBF, PBV, and MTT values were assessed using classical statistical analysis methods with the use of Student's coefficient for the corresponding confidence level.

RESULTS

MR perfusion data of 10 volunteers are presented in Tables 2–4. The passage time at the pulmonary trunk was lower than that of the lung parenchyma, since the pulmonary trunk is characterized by an almost constant volume, that is, blood flow is due only to hydrostatic pressure which value decreases

in the course of blood flow [3]. The passage times in the central and peripheral parts were approximately equal, the experimental data ranges overlapped, and the values obtained were somewhat higher than for the pulmonary trunk. The data obtained indicate that the capacitive characteristics of the vessels of the central and peripheral lobes of the lungs are approximately the same.

The PBF and PBV values (Tables 3 and 4) are lower in the peripheral regions, which, considering the data in Table 2, indicates that a decrease in PBF is due to a decrease in PBV and is graphically presented as a smaller range of intensity changes in the peripheral regions. This may be due to the involvement of large arterioles in the blood supply to the

Table 2 / Таблица 2

The obtained values of the average passage time of the contrast agent (MTT) in the selected areas of interest
Полученные значения среднего времени пассажа контрастного препарата (MTT) в выбранных зонах интереса

Area of interest / Зона интереса	Average value, sec / Среднее значение, с	Error rate, sec / Погрешность, с	Confidence probability / Доверительная вероятность
MTT total / MTT общее	7.15	1.20	0.68
MTT pulmonary trunk / MTT ствол легочной артерии	5.28	0.40	0.68
MTT of central regions of pulmonary lobes / MTT центральных отделов долей легкого	7.21	1.23	0.68
MTT of peripheral regions of pulmonary lobes / MTT периферических отделов долей легкого	7.15	1.28	0.68

Table 3 / Таблица 3

The obtained values of pulmonary tissue perfusion (PBF) in the selected areas of interest
Полученные значения перфузии легочной ткани (PBF) в выбранных зонах интереса

Area of interest / Зона интереса	Average value / Среднее значение	Error rate / Погрешность	Confidence probability / Доверительная вероятность	Minimum value / Минимальное значение	Maximum value / Максимальное значение
PBF in peripheral regions / PBF в периферических отделах	55.4	10.20	0.046	42.4	70.2
PBF in central regions / PBF в центральных отделах	102.61	11.81	0.046	74.3	166
PBF with ROI in coronal plane / PBF с ROI в корональной проекции	78.21	12.2	0.046	50	90

Table 4 / Таблица 4

The obtained values of blood flow volume per 100 ml of lung tissue (PBV) in the central and peripheral regions of lungs
Полученные значения объема кровотока на 100 мл легочной ткани (PBV) в центральных и периферических отделах легких

Lung regions / Отделы легких	PBV, ml/100 ml of lung tissue / PBV, мл/100 мл легочной ткани	Relative error / Относительная погрешность	Absolute error / Абсолютная погрешность
Central regions / Центральные отделы	12.33	0.21	2.54
Peripheral regions / Периферические отделы	6.60	0.31	2.04

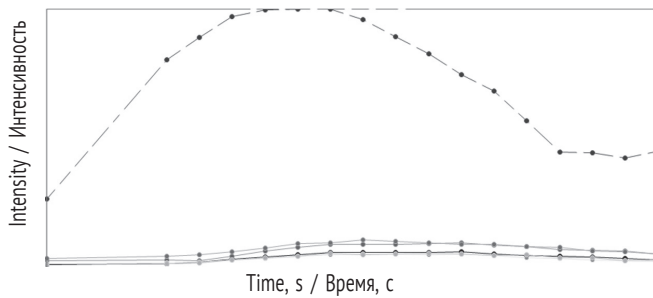


Fig. 3. Time-intensity curves in the area of interest. The signal received for ROI in the area of the pulmonary trunk is depicted as the dashed line. Other lines are the areas of interest selected in the pulmonary parenchyma. The image obtained with integrated FireVoxel tools

Рис. 3. Кривые зависимости интенсивности сигнала от времени в зоне интереса. Пунктирной линией отображается сигнал, полученный для ROI в области легочного ствола. Остальные линии – области интереса, выбранные в легочной паренхиме. Изображение получено встроенными средствами FireVoxel

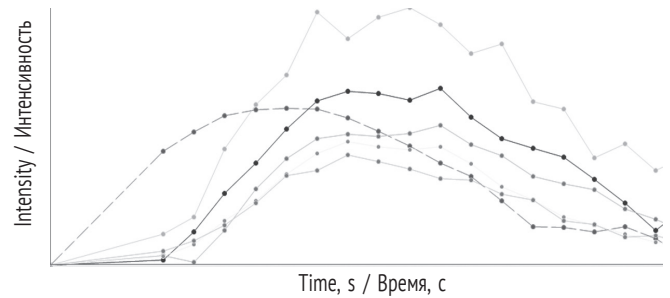


Fig. 4. Graphs of the dependence of the relative content of the contrast agent in the area of interest. The dashed line corresponds to the pulmonary trunk. Other lines reflect signal intensity in different ROI in pulmonary parenchyma

Рис. 4. Графики зависимости относительного содержания контрастного препарата в зоне интереса. Пунктирной линией обозначена зона интереса в области легочного ствола, остальные линии – зоны интереса, выбранные в легочной паренхиме

peripheral lobes, in the central parts of the lungs, but which, nevertheless, cannot be excluded from the examination zone because of their small caliber.

Thus, the results obtained demonstrate the feasibility of using 3D ultrafast dynamic contrast MRI to assess the difference in blood flow parameters in healthy lung tissues. Figures 3 and 4 present contrast curves (signal intensity versus time) and graphs of the relative level of the contrast agent in the area of interest. Figure 4 demonstrates that the use of semiquantitative methods with the calculation of relative contrast is somewhat incorrect, as the relative change in signal intensity for areas of the lung parenchyma may exceed that for the pulmonary trunk because of the heterogeneity of the lung tissue due to the presence of air cavities. In this case, the following approximation should be used:

$$C(t) \propto S(t) - S(0),$$

where C is the contrast agent concentration, S is the signal intensity, and t is the transit time of the contrast agent. Since the hematocrit level may differ for the pulmonary trunk, arteries, and arterioles of the lungs, this should be taken into account when calculating the relative concentration [13, 19].

DISCUSSION

Physiological foundations for constructing a mathematical model of lung perfusion

The pulmonary circulation contains the entire volume of cardiac output both at rest and under tension. At rest, the blood flow of the lungs is heterogeneous and directed to the lower zones; under tension, expansion occurs and previously unused

vessels are involved in the circulation [2]. Currently, each vessel is characterized by resistance and capacity. Pulmonary vascular resistance is defined as the ratio of the pressure difference in the pulmonary artery and the left atrium and the PBF velocity. However, PBF cannot be considered laminar, and pulmonary vessels are more likely to be capacitive than resistive [3]. Thus, the vascular resistance value will not be constant, which enables us to consider perfusion in terms of the theory of signal processing, considering the tissue characteristics as a transfer function.

Four zones of the lungs are usually distinguished, namely, West's functional zones that consider the presence of pressure as the cause of blood flow [42]. Accordingly, alveolar, pulmonary arterial, and pulmonary venous pressures are distinguished [4, 15, 16].

The size of West's zones has a close relationship with the body position and depth of inhalation. Figure 5 shows a schematic representation of West's zones, while zone 4 (areas of the lungs with reduced blood flow, where resistance to blood flow is created by extra-alveolar vessels) is not marked, as it disappears with deep inhalation [4]. In addition, in the prone position, most areas of the lungs correspond to zone 3; zone 1 is absent, and zone 2 is located in the anterior lung [5]; therefore, for the analysis of blood flow in healthy volunteers in this study (the study was conducted with the participants inhaling and lying on the back) the apex of the lungs was selected, where the pressure in the pulmonary artery is greater than the pulmonary venous pressure and, in turn, higher than the alveolar one. Thus, in this zone, the blood flow is determined by the difference between

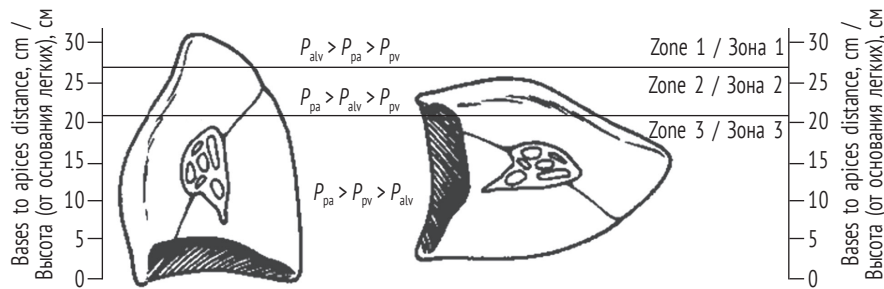


Fig. 5. Schematical representation of functional zones in the supine and standing positions [14]. P_{alv} – alveolar pressure; P_{pa} – pulmonary arterial pressure; P_{pv} – pulmonary venus pressure

Рис. 5. Схематическое изображение функциональных зон в положении лежа и стоя [14]. P_{alv} – альвеолярное давление; P_{pa} – давление легочное артериальное; P_{pv} – давление легочное венозное

the pressure in the pulmonary arteries and pulmonary veins, which justifies the usual calculations of pulmonary vascular resistance, previously discussed in detail by Axel [12]. An increase or decrease in blood flow in this area leads to the expansion of the already open capillaries [4]. Therefore, the zone of interest should be chosen while taking into account these aspects, and the most significant choice will be the choice of the zone of interest below the lung apex by 1–2 cm vertically.

The lung is an organ with a dual circulatory system. It has two arterial inputs: the first input, which functions in gas exchange, is through the system of pulmonary arteries and pulmonary veins, whereas the trophism of the organ is attributed to the bronchial arteries and veins. The bronchial arteries receive oxygenated blood from the systemic circulation, and the caliber of these vessels is rather small; therefore, the contribution of trophic blood flow is negligible because of small blood volumes and time delay [39].

By definition, perfusion is a physical nonmeasurable quantity that represents the volume of blood passing through 100 mL of the parenchyma of a particular tissue per minute. When analyzing CT and MRI data [12], the following parameters are usually used:

- PBV as PBF volume is the volume of blood passing through the selected area of interest during the monitoring period.
- MTT is the average time required for a contrast molecule or blood particles to reach the ROI.
- PBF as a value proportional to perfusion is the volume of blood that passes through the selected ROI per unit of time, normalized to its volume. This value is relative, as to calculate the exact values, hematological parameters of the blood should be measured, which can vary over a rather wide range and cannot be determined immediately before the examination.

The existing concept of the indicator dilution theory [28] uses the volume and velocity of blood flow per 100 mL of organ tissue to assess tissue perfusion, with minute as the unit of time; however, the average passage time is expressed in seconds.

$$C_{ROI}(t) = C_{AIF}(t) \otimes h(t) = \int_0^t C_{AIF}(\tau) \cdot h(t - \tau) d\tau,$$

where C is the concentration of the contrast agent, t is the monitoring period from the beginning of the contrast agent injection, h is the function corresponding to the distribution density of the time that particles pass to the study area over time, τ is the variable over which the integration is performed (the monitoring time from the beginning of the contrast agent injection), and d is the differential.

Several studies have proposed practical approaches for solving this equation and obtaining physiological parameters of interest from it [27, 33, 34] and are currently quite widespread when working with the central nervous system.

In addition, semiquantitative approaches can be used, as they consider function $h(t)$ as the probability for a particle to pass the ROI in time t and, accordingly, calculate the average passage time as the first moment of this function. Studies [28, 34, 35] have indicated that for further calculations, it is convenient to construct a transfer function as follows:

$$R(t) = 1 - \int_0^t h(\tau) d\tau$$

where R is the residual function, t is the monitoring period from the start of the injection of the contrast agent, h is the function corresponding to the distribution density of the particle transit time to the study area in time, τ is the variable over which the integration is performed (the monitoring time from the start of contrast agent injection), d is the differential, which can be performed both with and without the use of models [21, 30].

In calculations without using models, the matrix equation should be calculated [10]:

$$A \cdot b = c,$$

where matrix A and vector c are created from the input data, and vector b contains the transfer function and the value for blood flow velocity. To solve this equation, an algebraic approach with a singular value decomposition of the matrix A is used.

To obtain a graph of the dependence of the contrast agent concentration, we took into account the fact that, at its low concentrations, the concentration is directly proportional to the signal intensity [40]. To present the experimental data as desired, the following equation can be used:

$$C(t) \propto \frac{S(t)}{S(0)} - 1,$$

where C is the contrast agent concentration, S is the signal intensity, and t is the transit time of the contrast agent.

In the present study, we analyzed the dependence of signal intensity on time in the pulmonary artery and evaluated the dependence of signal intensity in the apexes of the lungs with the inclusion of gravity-dependent zones of the lungs. With this approach, the curve of dependence of the signal intensity in the selected area of interest on time is not approximated by any special function [1], for example, the AIF for the pulmonary trunk or the gamma function by analogy with the central nervous system.

When using a semiquantitative approach, the relative values of volume and blood flow are calculated using numerical integration methods; thus it is possible to determine the relative value of the blood volume, which is calculated as the area of the subgraph of the studied curve of the dependence of intensity on time obtained by the trapezoid method [6]. In this model, relative (i.e., in conditional) values of blood flow volume and velocity are obtained as results; however, the average transit time of the contrast agent is absolute.

In addition to the semiquantitative model, we used the method of calculating the blood flow velocity using the inverse convolution function and singular value decomposition of the matrix constructed from the intensity–time dependence plot for the pulmonary trunk, as demonstrated in [30], except for the fact that the concentration–intensity dependence was used to plot the curves for T1 images with a low concentration of contrast agent and was adjusted for hematocrit levels in large (pulmonary trunk) and small vessels (pulmonary artery branches, arterioles, etc.).

The forequoted findings of Hatabu et al. [18] were confirmed in the present study by numerical calculations. Table 3 presents PBF values that are consistent with previously obtained data from the world literature for coronal ROI selection [20]. The values obtained are within the experimental range.

The discrepancies in the data is possibly due to the possible introduction of a threshold value for the singular diagonal matrix in the calculations, which is used in the calculations [30]. In addition, some discrepancies in the reproducibility of results were demonstrated for this method [26]. In addition, by analogy with the central nervous system, with correction for the so-called contrast agent leakage [23], the model can be used for patients with interstitial lung diseases, which will be performed in further studies.

CONCLUSION

Thus, the model used has demonstrated its efficiency, and it can potentially be applied to patients with interstitial changes in the lungs.

ADDITIONAL INFORMATION

Author contributions. All authors confirm that their authorship complies with the ICMJE criteria. All authors have made a significant contribution to the development of the concept, research, and preparation of the article and have read and approved the final version before its publication.

Conflict of interest. The authors declare no conflict of interest.

Funding. The study had no external funding.

REFERENCES

1. Bagrov VG, Belov VV, Zadorozhnyy VN, et al. Metody matematicheskoy fiziki. III. Spetsial'nye funktsii Tomsk: Izd-vo NTL; 2002. 352 p. (In Russ.)
2. Gaydes MA. Regulyatsiya ventilyatsii i perfuzii v legkikh. *Medicina-Online.Ru*. 2006. (In Russ.) Режим доступа: <http://www.medicina-online.ru/articles/40247>.
3. German IP. The physics of humans body. Dolgoprudnyy: Intellekt; 2014. 991 p. (In Russ.)
4. Grippi MA. Patofiziologiya legkikh. 2nd ed. Moscow: Izdatel'stvo BINOM; 2016. 304 p. (In Russ.)
5. Dzgoev LB. Chetyrekhfaznaya model' dykhaniya (novoe v fiziologii dykhaniya cheloveka). *Vladikavkazskiy mediko-biologicheskiiy vestnik*. 2002;2(3):5–30. (In Russ.)
6. Zenkov A.V. Chislennyye metody. Moscow: Izdatel'stvo Yurayt, 2019. 122 p. (In Russ.)
7. Kolos AI, Saygel'dina LL, Zhaynorov NE, et al. Pulmonary arteriovenous shunt: the difficulty of diagnosis

- and treatment tactics. *Klinicheskaya Meditsina Kazakhstana*. 2015;(4(38)):74–78. (In Russ.)
8. Kondrashov VE, Korolev SB. MATLAB kak sistema programmirovaniya nauchno-tehnicheskikh raschetov Moscow: Mir, In-t strategicheskoy stabil'nosti Minatoma RF; 2002. 350 p. (In Russ.)
 9. Kontorovich MB, Zislin BD, Chistyakov AV, et al. The respiratory dead space and realization of physiological effects of high frequency stream pulmonary ventilation. *Kazan Medical journal*. 2009;90(3): 313–318. (In Russ.)
 10. Mamonov SS. Solving of matrix equations. *Bulletin of Ryazan State University Named For S.A. Yessenin*. 2009;1:115–136. (In Russ.)
 11. Naumenko ZhK, Chernyak AV, Neklyudova GV, et al. Ventilation-perfusion ratio. *Prakticheskaya Pul'monologiya*. 2018;(4):86–90. (In Russ.)
 12. Axel L. Cerebral blood flow determination by rapid-sequence computed tomography: theoretical analysis. *Radiology*. 1980;137(3):679–686. DOI: 10.1148/radiology.137.3.7003648
 13. Engblom H, Kanski M, Kopic S, et al. Importance of standardizing timing of hematocrit measurement when using cardiovascular magnetic resonance to calculate myocardial extracellular volume (ECV) based on pre- and post-contrast T1 mapping. *J Cardiovasc Magn Reson*. 2018;20(1):46. DOI: 10.1186/s12968-018-0464-9
 14. Fishman AP. Pulmonary diseases and disorders. 2nd ed. New York: McGraw-Hill, 1988.
 15. Hakim TS, Dean GW, Lisbona R. Effect of body posture on spatial distribution of pulmonary blood flow. *J Appl Physiol (1985)*. 1988;64(3):1160–1170. DOI: 10.1152/jappl.1988.64.3.1160
 16. Hakim TS, Lisbona R, Dean GW. Gravity-independent inequality in pulmonary blood flow in humans. *J Appl Physiol (1985)*. 1987;63(6):1114–1121. DOI: 10.1152/jappl.1987.63.6.1114
 17. Hatabu H, Gaa J, Kim D, et al. Pulmonary perfusion: qualitative assessment with dynamic contrast-enhanced MRI using ultra-short TE and inversion recovery turbo FLASH. *Magn Reson Med*. 1996;36(4):503–508. DOI: 10.1002/mrm.1910360402
 18. Hatabu H, Tadamura E, Levin DL, et al. Quantitative assessment of pulmonary perfusion with dynamic contrast-enhanced MRI. *Magn Reson Med*. 1999;42(6):1033–1038. DOI: 10.1002/(sici)1522-2594(199912)42:6<1033::aid-mrm7>3.0.co;2-7
 19. Hermann I, Uhrig T, Chacon-Caldera J, Akçakaya M. Towards measuring the effect of flow in blood T1 assessed in a flow phantom and *in vivo*. *Phys Med Biol*. 2020;65:095001.
 20. Janson N. Non-linear dynamics of biological systems. *Contemporary Physics*. 2012;53(2):137–168. DOI: 10.1080/00107514.2011.644441
 21. Jerosch-Herold M, Wilke N, Stillman AE. Magnetic resonance quantification of the myocardial perfusion reserve with a Fermi function model for constrained deconvolution. *Med Phys*. 1998;25(1):73–84. DOI: 10.1118/1.598163
 22. Kikuchi K, Murase K, Miki H, et al. Quantitative evaluation of mean transit times obtained with dynamic susceptibility contrast-enhanced MR imaging and with (133)Xe SPECT in occlusive cerebrovascular disease. *AJR Am J Roentgenol*. 2002;179(1):229–235. DOI: 10.2214/ajr.179.1.1790229
 23. Korfiatis P, Hu L, Kelm Z, et al. A DSC Digital Brain Phantom for Assessment of Leakage Correction Methods. Proceedings of the Radiological Society of North America and Scientific Assembly and Annual Meeting. 2013.
 24. Larsson HBW, Hansen AE, Berg HK, et al. Dynamic contrast-enhanced quantitative perfusion measurement of the brain using T1-weighted MRI at 3T. *J Magn Reson Imaging*. 2008;27(4):754–762. DOI: 10.1002/jmri.21328
 25. Levin DL, Chen Q, Zhang M, et al. Evaluation of regional pulmonary perfusion using ultrafast magnetic resonance imaging. *Magn Reson Med* 2001;46(1):166–171. DOI: 10.1002/mrm.1172
 26. Ley-Zaporozhan J, Molinari F, Risse F, et al. Repeatability and reproducibility of quantitative whole-lung perfusion magnetic resonance imaging. *J Thorac Imaging*. 2011;26(3):230–239. DOI: 10.1097/RTI.0b013e3181e48c36
 27. Malkov V, Rogers D, Jaffray D. TH-AB-BRA-05: Lung Cannot Be Treated as Homogeneous in Radiation Transport Simulations in Magnetic Fields. *Medical Physics*. 2016; 43(6):3854–3854.
 28. Meier P, Zierler KL. On the theory of the indicator-dilution method for measurement of blood flow and volume. *J Appl Physiol*. 1954;6(12):731–744. DOI: 10.1152/jappl.1954.6.12.731
 29. Murase K, Kikuchi K, Miki H, et al. Determination of arterial input function using fuzzy clustering for quantification of cerebral blood flow with dynamic susceptibility contrast-enhanced MR imaging. *J Magn Reson Imaging*. 2001;13(5):797–806. DOI: 10.1002/jmri.1111
 30. Murase K, Shinohara M, Yamazaki Y. Accuracy of deconvolution analysis based on singular value decomposition for quantification of cerebral blood flow using dynamic susceptibility contrast-enhanced magnetic resonance imaging. *Phys Med Biol*. 2001;46(12): 3147–3159. DOI: 10.1088/0031-9155/46/12/306
 31. Nyrén S, Mure M, Jacobsson H, et al. Pulmonary perfusion is more uniform in the prone than in the supine position: scintigraphy in healthy humans. *J Appl Physiol (1985)*. 1999;86:1135–1141. DOI: 10.1152/jappl.1999.86.4.1135

32. Ohno Y, Hatabu H, Takenaka D, et al. Contrast-enhanced MR perfusion imaging and MR angiography: utility for management of pulmonary arteriovenous malformations for embolotherapy. *Eur J Radiol.* 2002;41:136–146. DOI: 10.1016/s0720-048x(01)00419-3
 33. Ohno Y, Hatabu H, Takenaka D, et al. Solitary pulmonary nodules: potential role of dynamic MR imaging in management initial experience. *Radiology.* 2002;224(2):503–511. DOI: 10.1148/radiol.2242010992
 34. Ostergaard L, Sorensen AG, Kwong KK, et al. High resolution measurement of cerebral blood flow using intravascular tracer bolus passages. Part II: Experimental comparison and preliminary results. *Magn Reson Med.* 1996;36(5):726–736. DOI: 10.1002/mrm.1910360511
 35. Ostergaard L, Weisskoff RM, Chesler DA, et al. High resolution measurement of cerebral blood flow using intravascular tracer bolus passages. Part I: Mathematical approach and statistical analysis. *Magn Reson Med.* 1996;36:715–725.
 36. Pistolesi M, Miniati M, Di Ricco G, et al. Perfusion lung imaging in the adult respiratory distress syndrome. *J Thorac Imaging.* 1986;1(3):11–24. DOI: 10.1097/00005382-198607000-00004
 37. Schuster DP. ARDS: clinical lessons from the oleic acid model of acute lung injury. *Am J Respir Crit Care Med.* 1994;149(1):245–260. DOI: 10.1164/ajrccm.149.1.8111590
 38. Schuster DP, Kaplan JD, Gauvain K, et al. Measurement of regional pulmonary blood flow with PET. *J Nucl Med.* 1995;36(3):371–377.
 39. Wagner EM. Bronchial Circulation. *Encyclopedia of Respiratory Medicine.* 2006:255–259. DOI: 10.1016/B0-12-370879-6/00503-2
 40. Wake N, Chandarana H, Rusinek H, et al. Accuracy and precision of quantitative DCE-MRI parameters: How should one estimate contrast concentration? *Magn Reson Imaging.* 2018;52:16–23. DOI: 10.1016/j.mri.2018.05.007
 41. Weinmann HJ, Brasch RC, Press WR, et al. Characteristics of gadolinium-DTPA complex: a potential NMR contrast agent. *AJR Am J Roentgenol.* 1984;142(3):619–624. DOI: 10.2214/ajr.142.3.619
 42. West JB. Regional differences in the lung. *Chest.* 1978;74(4):426–437. DOI: 10.1378/chest.74.4.426
 43. Wilson JE, Bynum LJ, Ramanathan M. Dynamic measurement of regional ventilation and perfusion of the lung with Xe-133. *J Nucl Med.* 1977;18(7):660–668.
 44. Zhang LJ, Zhou CS, Schoepf UJ, et al. Dual-energy CT lung ventilation/perfusion imaging for diagnosing pulmonary embolism. *Eur Radiol.* 2013;23:2666–2675. DOI: 10.1007/s00330-013-2907-x
 45. Zierler K. Indicator dilution methods for measuring blood flow, volume, and other properties of biological systems: a brief history and memoir. *Ann Biomed Eng.* 2000;28(8):836–848. DOI: 10.1114/1.1308496
- СПИСОК ЛИТЕРАТУРЫ**
1. Багров В.Г., Белов В.В., Задорожный В.Н., и др. Методы математической физики. III. Специальные функции. Томск: Изд-во НТЛ, 2002. 352 с.
 2. Гайдес М.А. Регуляция вентиляции и перфузии в легких // *Medicina-Online.Ru.* 2006. Режим доступа: <http://www.medicina-online.ru/articles/40247/>
 3. Герман И.П. Физика организма человека: пер. с англ. Долгопрудный: Интеллект, 2014. 991 с.
 4. Гриппи МА. Патолофизиология легких. 2-е изд. Москва: Изд-во БИНОМ, 2016. 304 с.
 5. Дзгоев Л.Б. Четырехфазная модель дыхания (новое в физиологии дыхания человека) // *Владикавказский медико-биологический вестник.* 2002. Т. 2, № 3. С. 5–30.
 6. Зенков А.В. Численные методы. Москва: Юрайт, 2019. 122 с.
 7. Колос А.И., Сайгельдина Л.Л., Жайноров Н.Е., и др. Артериовенозные шунты легких: трудности диагностики и лечебной тактики // *Клиническая Медицина Казахстана.* 2015. № 4 (38). С. 74–78.
 8. Кондрашов В.Е., Королев С.Б. MATLAB как система программирования научно-технических расчетов. Москва: Мир, Ин-т стратегической стабильности Минатома РФ, 2002. 350 с.
 9. Конторович М.Б., Зислин Б.Д., Чистяков А.В., и др. Дыхательное мертвое пространство и реализация физиологических эффектов высокочастотной струйной вентиляции легких // *Казанский медицинский журнал.* 2009. Т. 90, № 3. С. 313–318.
 10. Мамонов СС. Решение матричных уравнений // *Вестник Рязанского государственного университета им. С.А. Есенина.* 2009. Т. 1. С. 115–136.
 11. Науменко Ж.К., Черняк А.В., Неклюдова Г.В., и др. Вентиляционно-перфузионное отношение // *Практическая пульмонология.* 2018. № 4. С. 86–90.
 12. Axel L. Cerebral blood flow determination by rapid-sequence computed tomography: theoretical analysis // *Radiology.* 1980. Vol. 137, No. 3. P. 679–686. DOI: 10.1148/radiology.137.3.7003648
 13. Engblom H., Kanski M., Kopic S., et al. Importance of standardizing timing of hematocrit measurement when using cardiovascular magnetic resonance to calculate myocardial extracellular volume (ECV) based on pre- and post-contrast T1 mapping // *J Cardiovasc Magn Reson.* 2018. Vol. 20, No. 1. P. 46. DOI: 10.1186/s12968-018-0464-9
 14. Fishman A.P. Pulmonary diseases and disorders. 2nd ed. New York: McGraw-Hill, 1988.
 15. Hakim T.S., Dean G.W., Lisbona R. Effect of body posture on spatial distribution of pulmonary blood flow // *J Appl Physiol* (1985). 1988. Vol. 64, No. 3. P. 1160–1170. DOI: 10.1152/jappl.1988.64.3.1160

16. Hakim T.S., Lisbona R., Dean G.W. Gravity-independent inequality in pulmonary blood flow in humans // *J Appl Physiol* (1985). 1987. Vol. 63, No. 3. P. 1114–1121. DOI: 10.1152/jappl.1987.63.3.1114
17. Hatabu H., Gaa J., Kim D., et al. Pulmonary perfusion: qualitative assessment with dynamic contrast-enhanced MRI using ultra-short TE and inversion recovery turbo FLASH // *Magn Reson Med*. 1996. Vol. 36, No. 4. P. 503–508. DOI: 10.1002/mrm.1910360402
18. Hatabu H., Tadamura E., Levin D.L., et al. Quantitative assessment of pulmonary perfusion with dynamic contrast-enhanced MRI // *Magn Reson Med*. 1999. Vol. 42, No. 6. P. 1033–1038. DOI: 10.1002/(sici)1522-2594(199912)42:6<1033::aid-mrm7>3.0.co;2-7
19. Hermann I., Uhrig T., Chacon-Caldera J., Akçakaya M. Towards measuring the effect of flow in blood T1 assessed in a flow phantom and *in vivo* // *Physics in Medicine and Biology*. 2020. Vol. 65. P. 095001.
20. Janson N. Non-linear dynamics of biological systems // *Contemporary Physics*. 2012. Vol. 53, No. 2. P. 137–168. DOI: 10.1080/00107514.2011.644441
21. Jerosch-Herold M., Wilke N., Stillman A.E. Magnetic resonance quantification of the myocardial perfusion reserve with a Fermi function model for constrained deconvolution // *Med Phys*. 1998. Vol. 25, No. 1. P. 73–84. DOI: 10.1118/1.598163
22. Kikuchi K., Murase K., Miki H et al. Quantitative evaluation of mean transit times obtained with dynamic susceptibility contrast-enhanced MR imaging and with (133)Xe SPECT in occlusive cerebrovascular disease // *AJR Am J Roentgenol*. 2002. Vol. 179, No. 1. P. 229–235. DOI: 10.2214/ajr.179.1.1790229
23. Korfiatis P., Hu L., Kelm Z., Erickson B. A DSC Digital Brain Phantom for Assessment of Leakage Correction Methods. Proceedings of the Radiological Society of North America and Scientific Assembly and Annual Meeting. 2013.
24. Larsson H.B.W., Hansen A.E., Berg H.K., et al. Dynamic contrast-enhanced quantitative perfusion measurement of the brain using T1-weighted MRI at 3T // *J Magn Reson Imaging*. 2008. Vol. 27, No. 4. P. 754–762. DOI: 10.1002/jmri.21328
25. Levin D.L., Chen Q., Zhang M., et al. Evaluation of regional pulmonary perfusion using ultrafast magnetic resonance imaging // *Magn Reson Med*. 2001. Vol. 46, No. 1. P. 166–171. DOI: 10.1002/mrm.1172
26. Ley-Zaporozhan J., Molinari F., Risse F., et al. Repeatability and reproducibility of quantitative whole-lung perfusion magnetic resonance imaging // *J Thorac Imaging* 2011. Vol. 26, No. 3. P. 230–239. DOI: 10.1097/RTI.0b013e3181e48c36
27. Malkov V., Rogers D., Jaffray D. TH-AB-BRA-05: Lung Cannot Be Treated as Homogeneous in Radiation Transport Simulations in Magnetic Fields // *Medical Physics*. 2016. Vol. 43, No. 6. P. 3854–3854.
28. Meier P., Zierler K.L. On the theory of the indicator-dilution method for measurement of blood flow and volume // *J Appl Physiol*. 1954. Vol. 6, No. 12. P. 731–744. DOI: 10.1152/jappl.1954.6.12.731
29. Murase K., Kikuchi K., Miki H., et al. Determination of arterial input function using fuzzy clustering for quantification of cerebral blood flow with dynamic susceptibility contrast-enhanced MR imaging // *J Magn Reson Imaging*. 2001. Vol. 13, No. 5. P. 797–806. DOI: 10.1002/jmri.1111
30. Murase K., Shinohara M., Yamazaki Y. Accuracy of deconvolution analysis based on singular value decomposition for quantification of cerebral blood flow using dynamic susceptibility contrast-enhanced magnetic resonance imaging // *Phys Med Biol*. 2001. Vol. 46, No. 12. P. 3147–3159. DOI: 10.1088/0031-9155/46/12/306
31. Nyrén S., Mure M., Jacobsson H., et al. Pulmonary perfusion is more uniform in the prone than in the supine position: scintigraphy in healthy humans // *J Appl Physiol* (1985). 1999. Vol. 86. P. 1135–1141. DOI: 10.1152/jappl.1999.86.4.1135
32. Ohno Y., Hatabu H., Takenaka D., et al. Contrast-enhanced MR perfusion imaging and MR angiography: utility for management of pulmonary arteriovenous malformations for embolotherapy // *Eur J Radiol*. 2002. Vol. 41. P. 136–146. DOI: 10.1016/s0720-048x(01)00419-3
33. Ohno Y., Hatabu H., Takenaka D., et al. Solitary pulmonary nodules: potential role of dynamic MR imaging in management initial experience // *Radiology*. 2002. Vol. 224, No. 2. P. 503–511. DOI: 10.1148/radiol.2242010992
34. Ostergaard L., Sorensen A.G., Kwong K.K., et al. High resolution measurement of cerebral blood flow using intravascular tracer bolus passages. Part II: Experimental comparison and preliminary results // *Magn Reson Med*. 1996. Vol. 36, No. 5. P. 726–736. DOI: 10.1002/mrm.1910360511
35. Ostergaard L., Weisskoff R.M., Chesler D.A., et al. High resolution measurement of cerebral blood flow using intravascular tracer bolus passages. Part I: Mathematical approach and statistical analysis // *Magn Reson Med*. 1996. Vol. 36, No. 5. P. 715–725. DOI: 10.1002/mrm.1910360510
36. Pistolesi M., Miniati M., Di Ricco G., et al. Perfusion lung imaging in the adult respiratory distress syndrome // *J Thorac Imaging*. 1986. Vol. 1, No. 3. P. 11–24. DOI: 10.1097/00005382-198607000-00004
37. Schuster D.P. ARDS: clinical lessons from the oleic acid model of acute lung injury // *Am J Respir Crit Care Med*. 1994. Vol. 149, No. 1. P. 245–260. DOI: 10.1164/ajrccm.149.1.8111590
38. Schuster D.P., Kaplan J.D., Gauvain K., et al. Measurement of regional pulmonary blood flow with PET // *J Nucl Med*. 1995. Vol. 36, No. 3. P. 371–377.
39. Wagner E.M. Bronchial Circulation // *Encyclopedia of Respiratory Medicine*. 2006. P. 255–259. DOI: 10.1016/B0-12-370879-6/00503-2

40. Wake N., Chandarana H., Rusinek H., et al. Accuracy and precision of quantitative DCE-MRI parameters: How should one estimate contrast concentration? // *Magn Reson Imaging*. 2018. Vol. 52. P. 16–23. DOI: 10.1016/j.mri.2018.05.007
41. Weinmann H.J., Brasch R.C., Press W.R., et al. Characteristics of gadolinium-DTPA complex: a potential NMR contrast agent // *AJR Am J Roentgenol*. 1984. Vol. 142, No. 3. P. 619–624. DOI: 10.2214/ajr.142.3.619
42. West J.B. Regional differences in the lung // *Chest*. 1978. Vol. 74, No. 4. P. 426–437. DOI: 10.1378/chest.74.4.426
43. Wilson J.E., Bynum L.J., Ramanathan M. Dynamic measurement of regional ventilation and perfusion of the lung with Xe-133 // *J Nucl Med*. 1977. Vol. 18, No. 7. P. 660–668.
44. Zhang L.J., Zhou C.S., Schoepf U.J., et al. Dual-energy CT lung ventilation/perfusion imaging for diagnosing pulmonary embolism // *Eur Radiol*. 2013. Vol. 23, No. 10. P. 2666–2675. DOI: 10.1007/s00330-013-2907-x
45. Zierler K. Indicator dilution methods for measuring blood flow, volume, and other properties of biological systems: a brief history and memoir // *Ann Biomed Eng*. 2000. Vol. 28, No. 8. P. 836–848. DOI: 10.1114/1.1308496

◆ Information about the authors

Anna V. Zakharova – Assistant Professor of the Department of Medical Biophysics. St. Petersburg State Pediatric Medical University, Ministry of Healthcare of the Russian Federation, Saint Petersburg; Radiologist, Department of Radiology Diagnostics of St. Petersburg State Medical Institution “City Multidisciplinary Hospital No. 2”, Saint Petersburg, Russia. E-mail: ellin-ave@yandex.ru.

Victoria V. Prits – Medical Physicist, Department of Radiology Diagnostics of St. Petersburg State Medical Institution “City Mariinsky Hospital”, Saint Petersburg, Russia. E-mail: brockendex.666@gmail.com

Alexander V. Pozdnyakov – MD, PhD, Dr. Med. Sci., Professor, Head of the Department of Radiology Diagnostic. St. Petersburg State Pediatric Medical University, Ministry of Healthcare of the Russian Federation, Saint Petersburg, Russia. E-mail: pozdnyakovalex@yandex.ru

◆ Информация об авторах

Анна Валерьевна Захарова – ассистент кафедры медицинской биофизики, ФГБОУ ВО «Санкт-Петербургский государственный педиатрический медицинский университет» Минздрава России, Санкт-Петербург; врач-рентгенолог отдела лучевой диагностики, СПбГБУЗ «Городская многопрофильная больница № 2», Санкт-Петербург, Россия. E-mail: ellin-ave@yandex.ru

Виктория Владимировна Приц – медицинский физик отделения лучевой диагностики. СПбГБУЗ «Городская Мариинская больница», Санкт-Петербург, Россия. E-mail: brockendex.666@gmail.com

Александр Владимирович Поздняков – д-р мед. наук, профессор, заведующий отделением лучевой диагностики. ФГБОУ ВО «Санкт-Петербургский государственный педиатрический медицинский университет» Минздрава России, Санкт-Петербург, Россия. E-mail: pozdnyakovalex@yandex.ru